

Supporting Information

Photosensitized electron transfer within self-assembled *norharmane/2'-deoxyadenosine 5'-monophosphate (dAMP)* complex

M. Micaela Gonzalez^a, Federico A. O. Rasse-Suriani^b, Carlos A. Franca^c, Reinaldo Pis Diez^c, Yousef Gholipour^d, H. Nonami^d, Rosa Erra-Balsells^{a} and Franco M. Cabrerizo^{b*}*

^a CIHDECAR - CONICET, Departamento de Química Orgánica, Facultad de Ciencias Exactas y Naturales, Universidad de Buenos Aires, Pabellón 2, 3p, Ciudad Universitaria, (1428) Buenos Aires, Argentina. E-mail: erra@qo.fcen.uba.ar

^b IIB-INTECH-UNSAM-CONICET (sede Chascomús). Intendente Marino Km 8,2. CC 164, (7130) Chascomús, Argentina. E-mail: fcabrerizo@intech.gov.ar

^c CEQUINOR - CONICET, Facultad de Ciencias Exactas, Universidad Nacional de la Plata, calle 47 y 115, (1900) La Plata, Argentina.

^d Plant Biophysics/Biochemistry Research Laboratory, College of Agriculture, Ehime University, 3-5-7 Tarumi, (790-8566) Matsuyama, Japan.

* To whom correspondence should be addressed.

Contents:

1. UV-vis spectrophotometric titration at pH 2.5 and 10.5. (Page S3)
2. ^1H -NMR spectra of nHoH $^+$ as a function of the βC concentration. (Page S4)
3. ^1H -NMR spectra. Chemical shift of C2-H and C8-H protons of H(dAMP) $^-$ as a function of the nucleotide concentration. (Page S5)
4. Quenching of *norharmane* fluorescence by dAMP: steady state analysis. (Page S6)
5. Quenching of *norharmane* fluorescence by dAMP: time-resolved analysis. (Page S7)
6. Stern-Volmer plots for quenching of *norharmane* fluorescence by dAMP. (Page S8)
7. Kinetic analysis of the dAMP oxidation photosensitized by *norharmano* under alkaline aqueous solution: HPLC data. (Page S9)
8. Numerical support: role of $^1\text{O}_2$ in the photosensitized reaction of dAMP. (Page S10)
9. ESI mass spectrometry analysis. (Page S11)
10. UV-LDI-TOF mass spectrometry analysis. (Page S13)
11. Typical fragmentation pattern of [dAMPO₄H₃] $^+$ and [8-oxodAMPO₄H₃] $^+$. (Page S15)
12. Hydrogen Bond assignations for complex S2.5, S5.4 and S10.5. (Page S16)

1. UV-vis spectrophotometric titration at pH 2.5 and 10.5

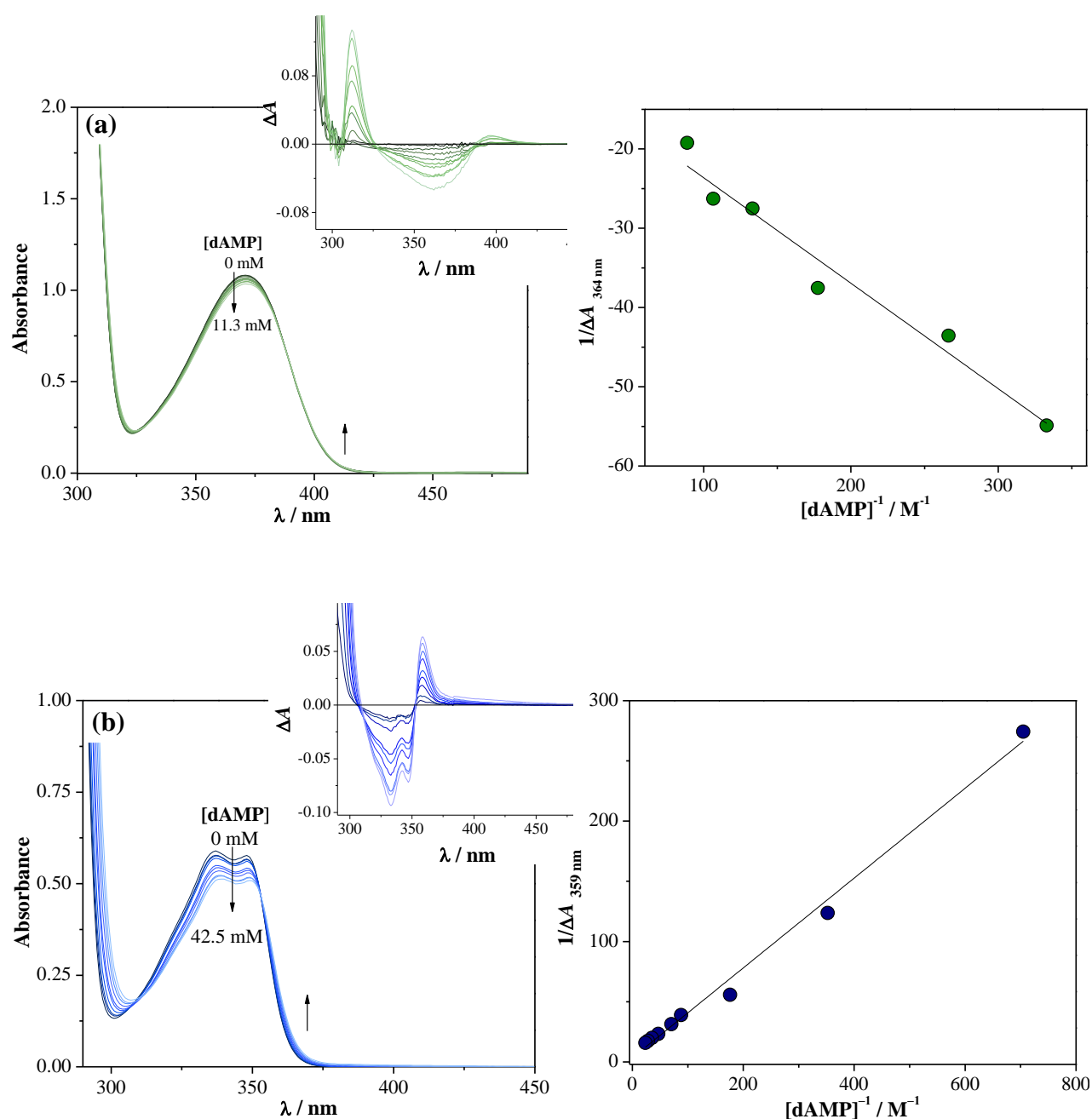


Figure SI.1. UV-vis absorption spectra of *norharmane* in the presence of increasing amounts of dAMP (see arrows). *Inset:* a representative Benesi-Hildebrand plots for each case. (a) pH 2.5, $[\text{nHoH}^+] = 2.6 \times 10^{-4} \text{ M}$ and (b) pH 10.5, $[\text{nHoN}] = 1.5 \times 10^{-4} \text{ M}$.

2. $^1\text{H-NMR}$ spectra of nHoH $^+$ as a function of the βC concentration

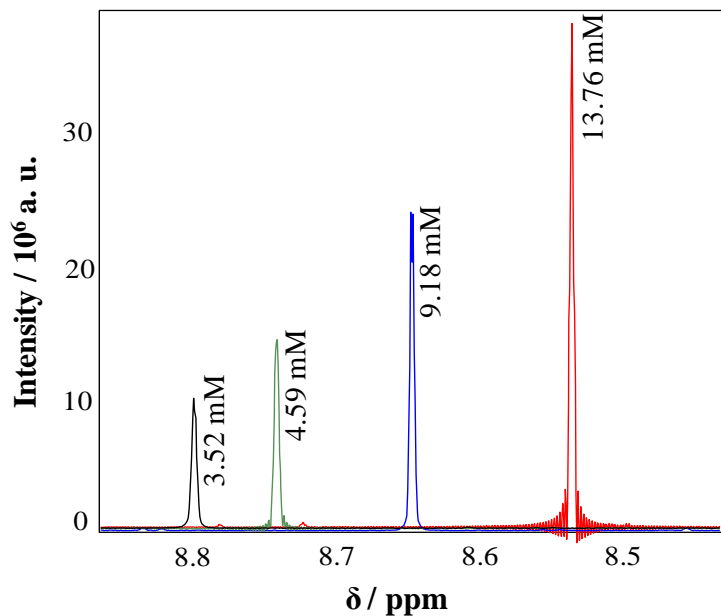


Figure SI.2. Representative example of the chemical shift as a function of norharmane concentration for C1-H in D₂O solution at pD 5.0. To show the changes, four different $^1\text{H-NMR}$ spectra are overlapped in the same plot.

Table SI.1. Values of self-association constant ($K_{\text{aa}}^{\text{nHoD}^+}$), critic concentration for aggregation (c.a.c.) and number of molecules per aggregates (n) obtained for nHoD $^+$ (D₂O, pD 5.0) from the analysis of the chemical shift of different protons. δ_m and δ_{agg} represent the chemical shift for a given proton in the monomer and in the homo-complex, respectively.

nHoD $^+$ proton (pD 5.0)	δ_m / ppm	δ_{agg} / ppm	c.a.c. / mM	n	$K_{\text{aa}}^{\text{nHoH}^+}$ / M $^{-1}$	$\langle K_{\text{aa}}^{\text{nHoH}^+} \rangle$ / M $^{-1}$
C1-H	8.975 ± 0.009	8.1 ± 0.3	4.4	$1.7 \sim 2$	6 ± 1	
C4-H	8.558 ± 0.008	7.7 ± 0.2	2.7	$1.7 \sim 2$	6 ± 2	
C6-H	7.45 ± 0.01	7.1 ± 0.2	4.2	$1.7 \sim 2$	6 ± 1	7 ± 1
C7-H	7.78 ± 0.01	7.4 ± 0.3	4.5	$1.8 \sim 2$	8 ± 2	

3. ^1H -NMR spectra. Chemical shift of C2-H and C8-H protons of $\text{H}(\text{dAMP})^-$ as a function of the nucleotide concentration

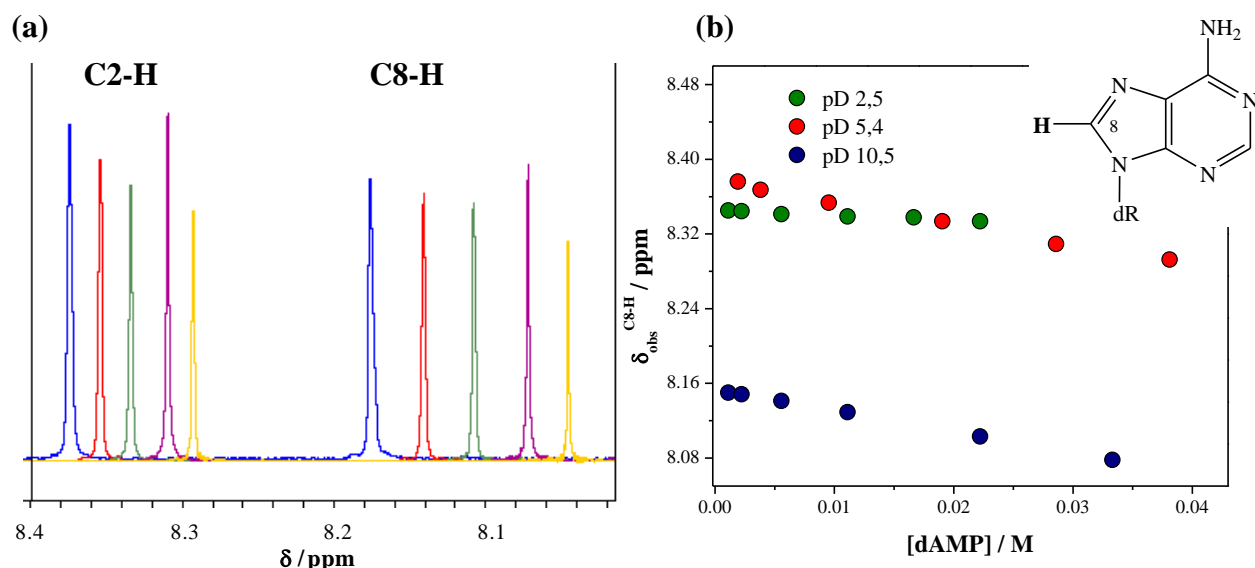


Figure SI.3. (a) Representative example of the chemical shift as a function of nucleotide concentration for C2-H and C8-H in D_2O solution at pD 5.4. To show the changes, five different ^1H -NMR spectra are overlapped in the same plot. (b) Evolution of the chemical shift (δ , in ppm) of nucleotide C8-H under three different pD conditions.

Table SI.2. Values of self-association constant ($K_{\text{aa}}^{\text{H}(\text{dAMP})^-}$), critic concentration for aggregation (c.a.c.) and number of molecules per aggregates (n) obtained for $\text{H}(\text{dAMP})^-$ (D_2O , pD 5.4) from the analysis of the chemical shift of different protons. δ_m and δ_{agg} represent the chemical shift for a given proton in the monomer and in the homo-complex, respectively.

$\text{H}(\text{dAMP})^-$ proton (pD 5.4)	δ_m / ppm	δ_{agg} / ppm	c.a.c. / mM	n	$K_{\text{aa}}^{\text{H}(\text{dAMP})^-}$ / M^{-1}	$\langle K_{\text{aa}}^{\text{H}(\text{dAMP})^-} \rangle$ / M^{-1}
C2-H	8.378 ± 0.002	7.7 ± 0.3	12.1	$1.9 \sim 2$	1.1 ± 0.1	
C8-H	8.181 ± 0.002	7.5 ± 0.2	8.1	$2.0 \sim 2$	2.6 ± 0.9	1.7 ± 0.8
C2'-H	6.441 ± 0.002	5.8 ± 0.2	11.9	$1.9 \sim 2$	1.4 ± 0.6	

Chemical structure of dAMP: A deoxyribose sugar attached to an adenine base. Adenine is a purine ring system with an amino group (NH_2) at position 6 and a carbonyl group at position 2.

4. Quenching of *norharmane* fluorescence by dAMP: steady state analysis

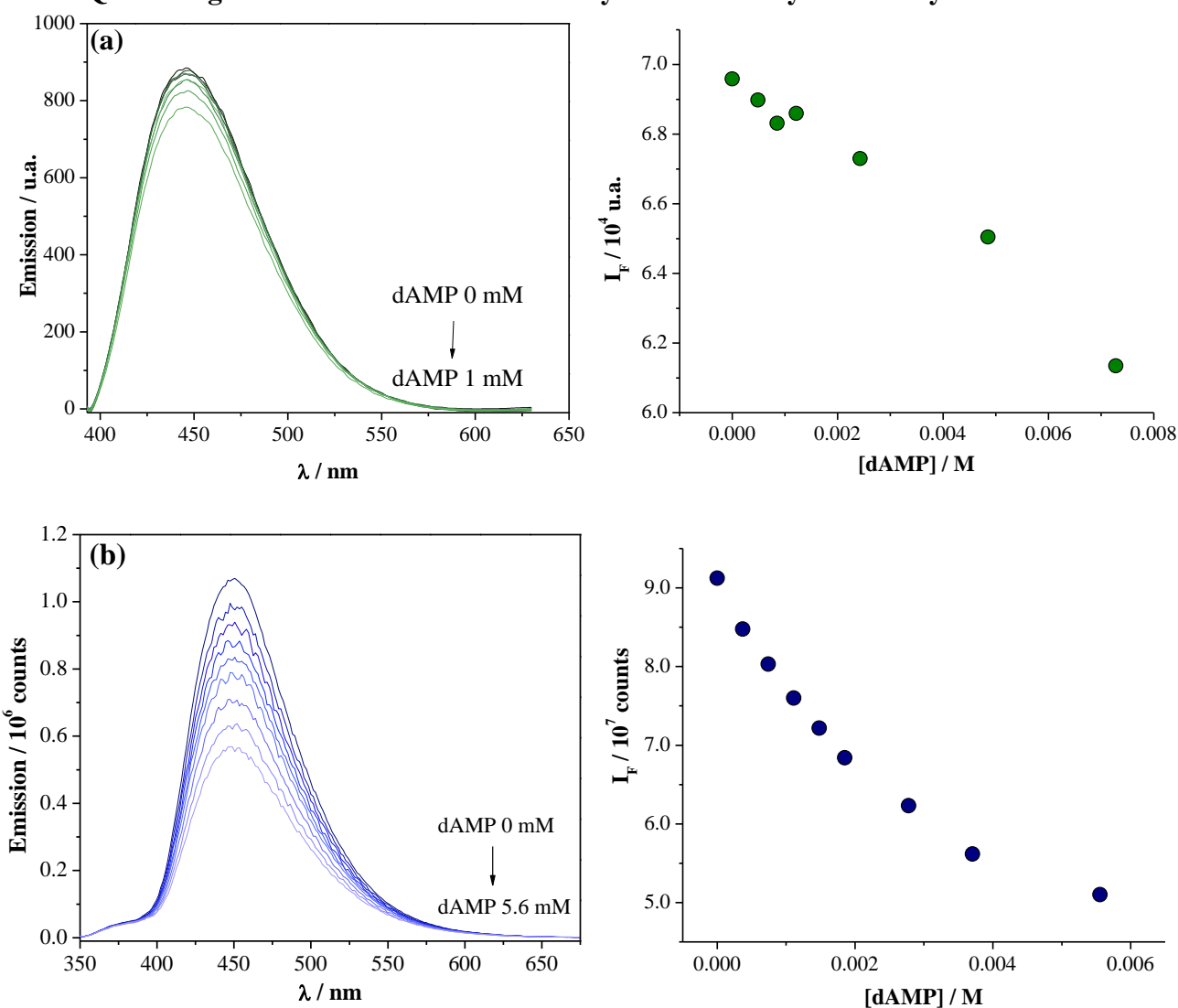


Figure SI.4. Corrected fluorescence spectra of *norharmane* aqueous solution (2.0×10^{-5} M) as a function of the dAMP concentrations: (a) pH 2.5, $\lambda_{\text{exc}} = 380$ nm, $\lambda_{\text{em}} = 383$ -680 nm and (b) pH 10.5, $\lambda_{\text{exc}} = 345$ nm, $\lambda_{\text{em}} = 350$ -680 nm.

5. Quenching of *norharmane* fluorescence by dAMP: time-resolved analysis

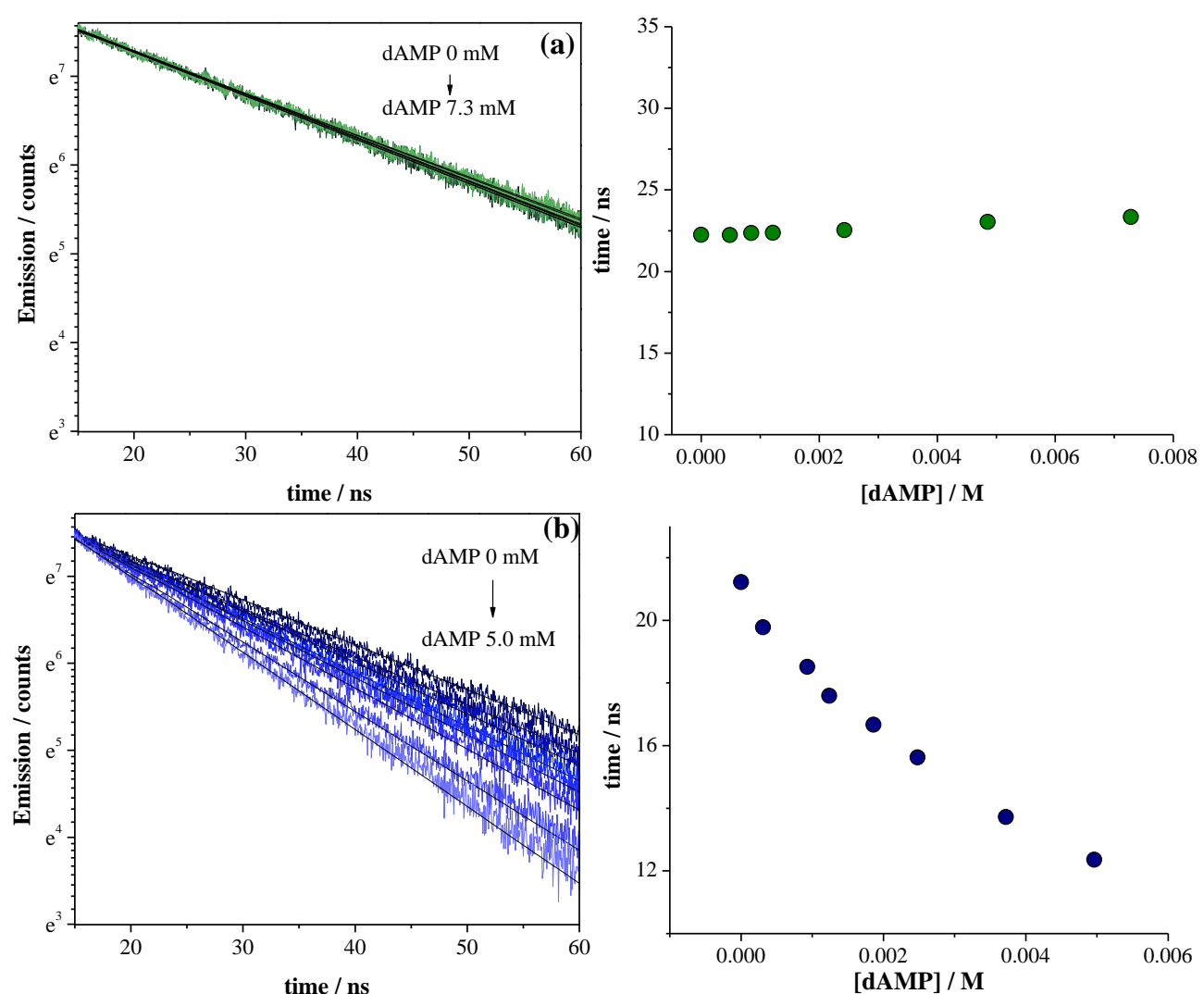


Figure SI.5. Fluorescence decays of *norharmane* aqueous solution (2.0×10^{-5} M) as a function of the dAMP concentrations at pH (a) 2.5, (b) 5.4 and (c) 10.5. $\lambda_{\text{exc}} = 341$ nm, $\lambda_{\text{em}} = 450$ nm.

6. Stern-Volmer plots for quenching of *norharmane* fluorescence by dAMP

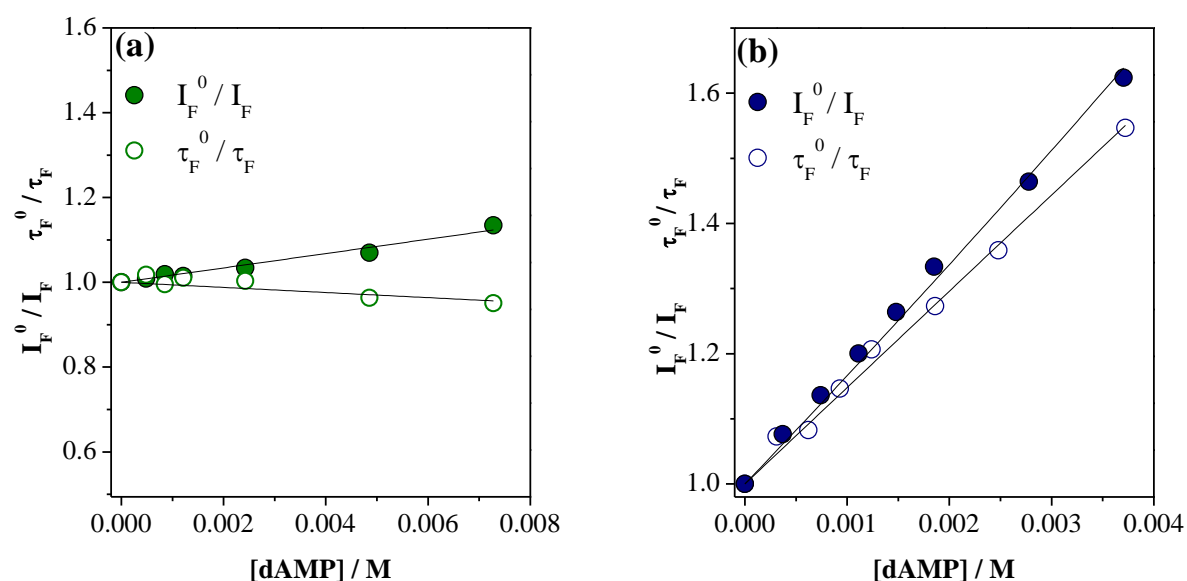


Figure SI.6. Quenching of *norharmane* fluorescence by dAMP at pH: (a) 2.5 and (b) 10.5. Stern–Volmer plots of the fluorescence intensities (I_F) and the fluorescence lifetimes (τ_F); $\lambda_{\text{exc}} = 341$ nm, $\lambda_{\text{em}} = 450$ nm.

7. Kinetic analysis of the dAMP oxidation photosensitized by norharmane under alkaline aqueous solution. HPLC data

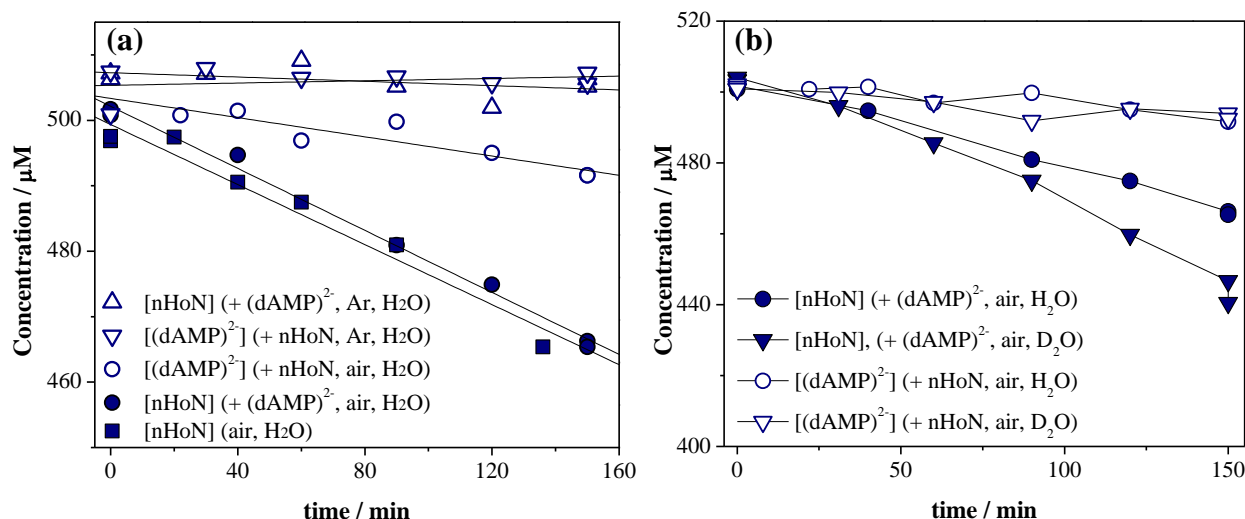


Figure SI.7. HPLC analysis: evolution of the $(\text{dAMP})^{2-}$ and nHoN concentration as a function of irradiation time ($\lambda_{\text{exc}} = 350 \pm 15 \text{ nm}$). **(a)** Experiments performed in alkaline aqueous solutions under different atmospheric conditions. “+” means “in the presence of”. **(b)** Comparison between experiments performed in alkaline aqueous and D₂O solutions, $\lambda_{\text{exc}} = 350 \pm 15 \text{ nm}$ and pH or pD 10.5. “+” means “in the presence of”.

8. Numerical support: role of $^1\text{O}_2$ in the photosensitized reaction of dAMP

The contribution of $^1\text{O}_2$ to the photosensitized oxidation of dAMP by *norharmane* can be evaluated by comparing the experimental initial rate of dAMP consumption to the initial rate of the reaction between $^1\text{O}_2$ and dAMP calculated from:

$$v = -d[\text{dAMP}]/dt = k_r [\text{dAMP}]_0 [^1\text{O}_2]_{\text{EE}} \quad (\text{SI.1})$$

where k_r is the rate constant of the chemical reaction between $^1\text{O}_2$ and dAMP ($(8 \pm 3) \times 10^3 \text{ L mol}^{-1} \text{ s}^{-1}$)¹, $[\text{dAMP}]_0$ is the initial nucleotide concentration and $[^1\text{O}_2]_{\text{EE}}$ is the steady-state concentration of singlet oxygen, that can be estimated from the following equation:

$$[^1\text{O}_2]_{\text{EE}} = (P_a \Phi_\Delta) / (k_d + k_t [\text{dAMP}]) \quad (\text{SI.2})$$

where P_a the photon flux absorbed by the singlet oxygen photosensitizer (*i. e.*, *norharmane*) and Φ_Δ is the quantum yield of $^1\text{O}_2$ production by the alkaloid (0.10 or 0.08 in acidic and alkaline solution, respectively),² k_d is the rate constant of $^1\text{O}_2$ deactivation by de solvent ($\tau_\Delta^{-1} = \sim 4^{-1} \mu\text{s}^{-1}$) and k_t is the rate constant for the total deactivation of $^1\text{O}_2$ by dAMP ($(4.1 \pm 0.4) \times 10^5 \text{ L mol}^{-1} \text{ s}^{-1}$)¹

Assuming that k_r in H_2O are similar to that determined in D_2O (no deuterium isotopic effect), under both pH conditions,³ a value of $7 \times 10^{-4} \mu\text{M min}^{-1}$ and $5 \times 10^{-4} \mu\text{M min}^{-1}$ were calculated for the initial rate of the reaction between $^1\text{O}_2$ and dAMP ($[\text{dAMP}]_0 = 500 \mu\text{M}$) under acidic and alkaline solution, respectively.

1 G. Petroselli, R. Erra-Balsells, F. M. Cabrerizo, C. Lorente, A. L. Capparelli, A. M. Braun, E. Oliveros and A. H. Thomas, *Org. Biomol. Chem.*, 2007, **5**, 2792–2799.

2 M. M. Gonzalez, M. L. Salum, Y. Gholipour, F. M. Cabrerizo and R. Erra-Balsells, *Photochem. Photobiol. Sci.*, 2009, **8**, 1139–1149.

3 The rate constant of the reaction between $^1\text{O}_2$ and dAMP (k_r) was only determined in D_2O solution at pD 5.5.

9. ESI mass spectrometry analysis.

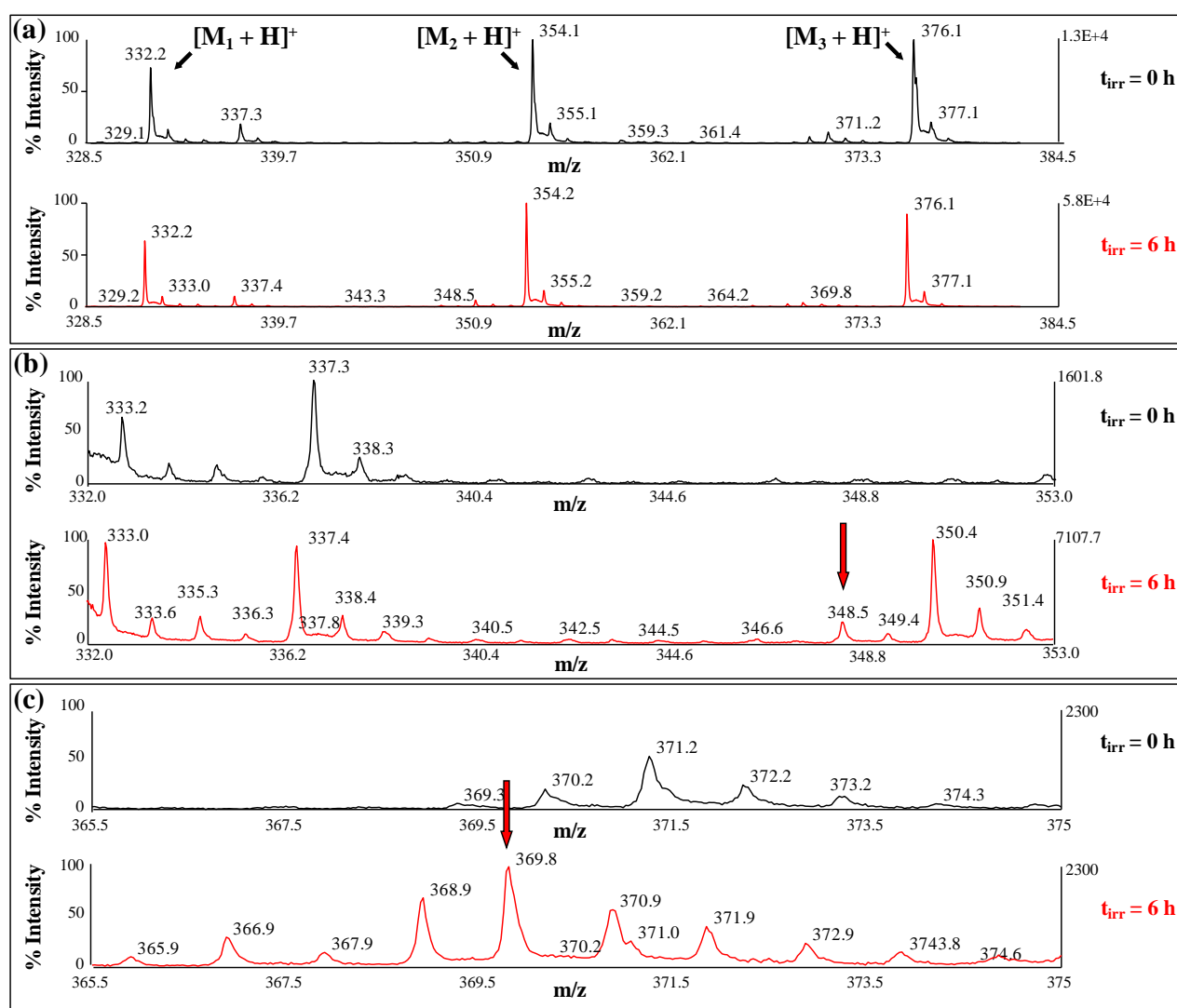


Figure SI.8. (a) ESI mass spectra of a irradiated (for 6 h, at 350 nm) and non-irradiated solution containing the system nHoH⁺/H(dAMP)⁻ (pH 5.4). Analysis carried out in positive ion mode. (b) and (c) are amplifications of three different regions of (a) to better visualize the acquired signals. Red arrows indicate the signals corresponding to 8-oxodAMP adducts.

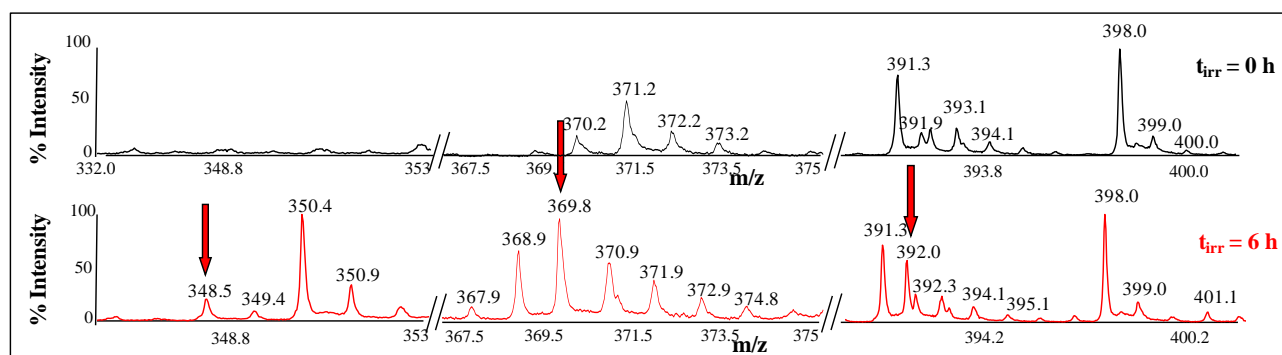


Figure SI.9. Amplification of different regions of the ESI mass spectra of a irradiated (for 6 h, at 350 nm) and non-irradiated solution containing the system $\text{nHoH}^+/\text{H(dAMP)}^-$ (pH 5.4). Analysis carried out in positive ion mode. Red arrows indicate the signals corresponding to 8-oxodAMP adducts.

10. UV-LDI-TOF mass spectrometry analysis.

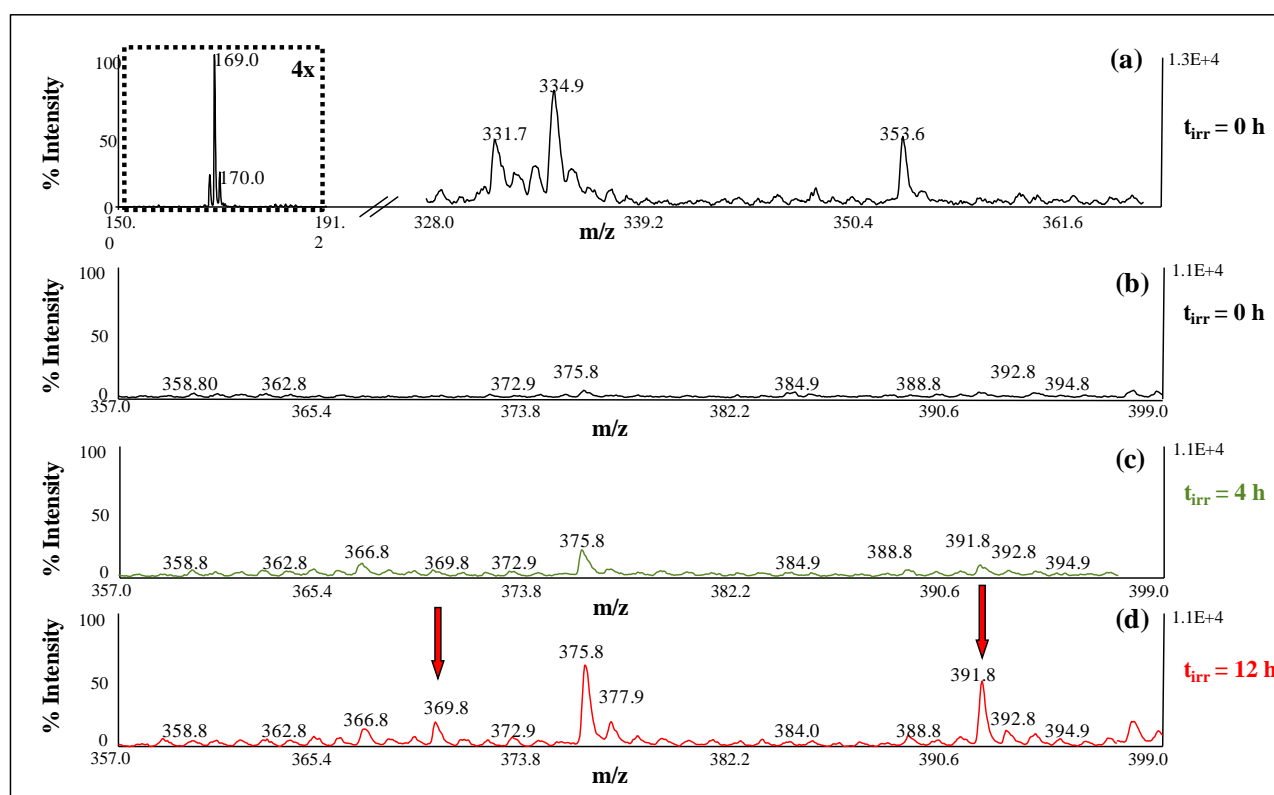


Figure SI.10. UV-LDI-TOF mass spectra of a irradiated (for 6 h, at 350 nm) and non-irradiated solution containing the system S5.4 ($\text{nHoH}^+ / \text{H(dAMP)}^-$, at pH 5.4). Analysis carried out in positive ion mode. (a) and (b) shows different regions of the same spectra corresponding to a non-irradiated solution. In figure (a), the intensity scale of the part of the spectra above $m/z = 192$ (see region inside the dashed lines) is reduced 4 times, to better show nucleotide signals. (c) and (d) show UV-LDI-TOF mass spectra of irradiated solutions during 4 and 12 h, respectively. Red arrows indicate the signals corresponding to 8-oxodAMP adducts.

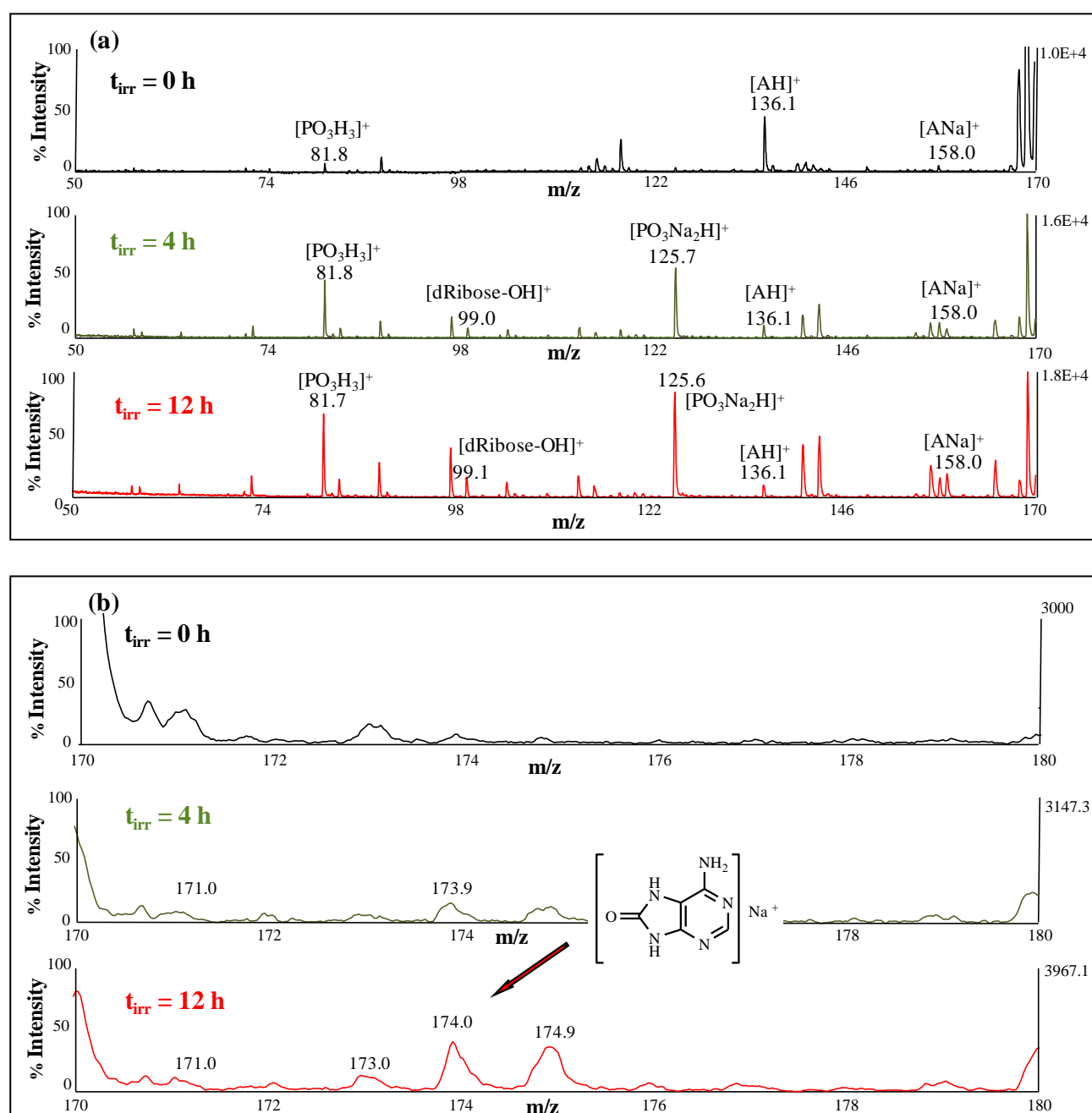
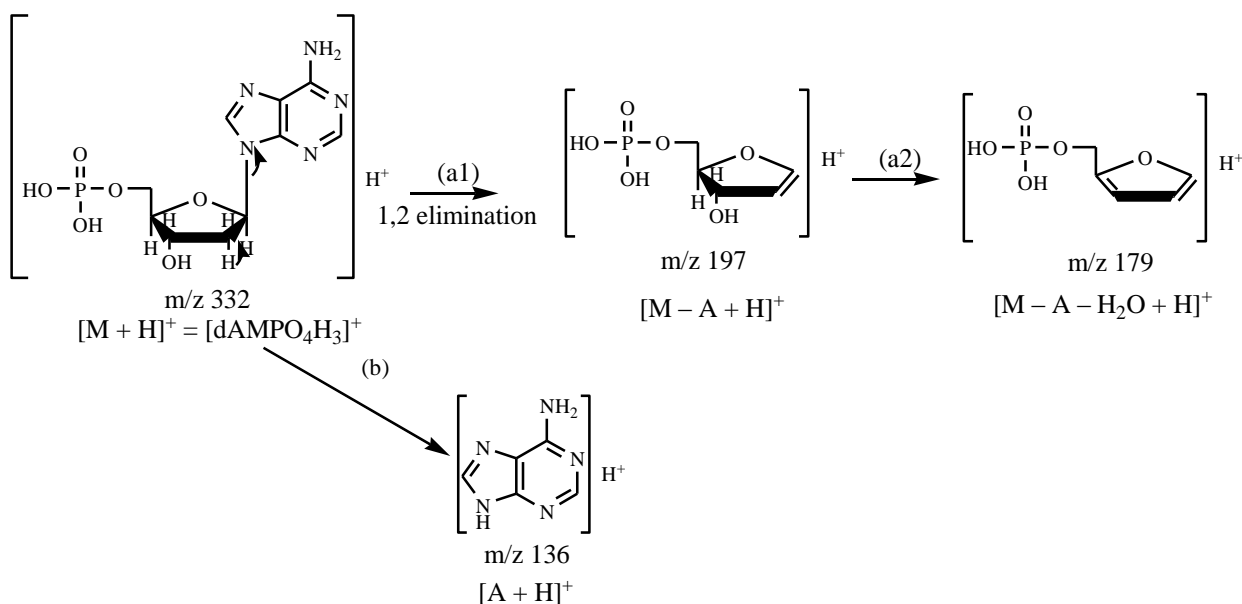


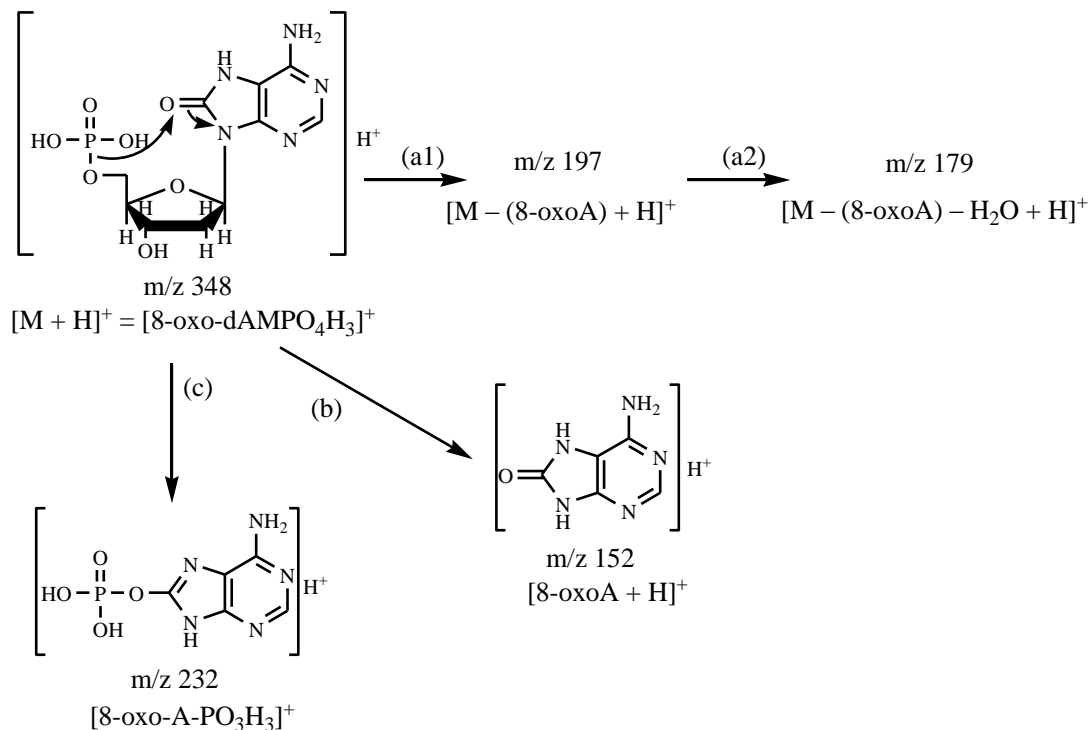
Figure SI.11. UV-LDI-TOF mass spectra of non-irradiated ($t_{\text{irr}} = 0 \text{ h}$) and irradiated ($t_{\text{irr}} = 4 \text{ and } 12 \text{ h}$, $\lambda_{\text{exc}} = 350 \pm 15 \text{ nm}$) aqueous solution of $\text{H}(\text{dAMP})^-$ and nHoH^+ (pH 5.4). Analysis carried out in positive ion mode. **(a)** and **(b)** shows different m/z region of the same spectra. Inset: chemical structure of the fragment $[8\text{-oxo-ANa}]^+$ formed from 8-oxodAMP.

11. Typical fragmentation pattern of $[dAMPO_4H_3]^+$ and $[8\text{-oxodAMPO}_4H_3]^+$.

(a)



(b)



Scheme SI.1. Typical fragmentation pattern of: (a) $[dAMPO_4H_3]^+$ and (b) $[8\text{-oxodAMPO}_4H_3]^+$.

12. Hydrogen Bond assignations for complex S2.5, S5.4 and S10.5.

Table SI.4: Hydrogen Bond assignations for complex S2.5.

Conformer	Bond type X—H···Y	Length (Å)		Angle X—H···Y
		X—H	H···Y	
1	9N—H···O (HPO ₄)	1.036	1.928	153.8°
	(OH) O—H···O (PO ₄)	1.033	1.713	153.6°
	1C—H···O (desoxyribose)	1.109	2.196	129.1°
2	(HPO ₄) O—H···O (OH)	1.024	1.749	165.3°
3	2N—H···O (PO ₄)	1.093	1.615	157.8°
	8C—H···O (PO ₄)	1.105	1.978	154.5°
4	9N—H···O (desoxyribose)	1.027	1.896	156.7°
	(HPO ₄) O—H···O (OH)	1.023	1.757	164.6°
5	2N—H···O (PO ₄)	1.099	1.57	177.2°
6	2N—H···O (PO ₄)	1.100	1.579	167.6°
	(HPO ₄) O—H···O (desoxyribose)	1.019	1.749	151.1°
	8C—H···O (ester)	1.095	2.038	128.3°
7	2N—H···O (PO ₄)	1.098	1.575	167.7°
	8C—H···O (ester)	1.096	2.075	159.0°
8	2N—H···O (PO ₄)	1.101	1.577	165.1°
	8C—H···O (ester)	1.096	2.041	145.0°
9	(HPO ₄) O—H···O (OH)	1.029	1.700	168.0°
10	9N—H···O (HPO ₄)	1.036	1.793	175.6°
12	(OH) O—H···O (PO ₄)	1.035	1.659	163.5°
13	9N—H···O (HPO ₄)	1.057	1.663	170.0°
	1C—H···O (HPO ₄)	1.112	1.979	155.2°
	3'C—H···O (PO ₄)	1.113	2.182	153.0°
14	(HPO ₄) O—H···O (OH)	1.025	1.784	155.6°
15	(HPO ₄) O—H···O (OH)	1.020	1.775	156.5°
16	2N—H···O (PO ₄)	1.099	1.571	159.2°
17	2N—H···O (PO ₄)	1.09	1.621	152.3°
	(HPO ₄) O—H···O (desoxyribose)	1.013	1.743	151.9°
18	2N—H···O (HPO ₄)	1.064	1.744	162.7°

Table SI.5: Hydrogen Bond assignations for complex S5.4.

Conformer	Bond type X—H···Y	Length (Å)		Angle X—H···Y
		X—H	H···Y	
1	9N—H···O (HPO ₄)	1.057	1.671	173.8°
	(HPO ₄) O—H···O (desoxyribose)	1.020	1.724	146.2°
	8C—H···O (PO ₄)	1.092	2.140	159.8°
2	2N—H···O (PO ₄)	1.094	1.604	163.2°
3	2N—H···O (PO ₄)	1.094	1.601	167.8°
	10C—H···O (HPO ₄)	1.109	2.087	137.4°

Table SI.6: Hydrogen Bond assignations for complex S10.5.

Conformer	Bond type X—H···Y	Length (Å)		Angle X—H···Y
		X—H	H···Y	
1	9N—H···O (desoxyribose)	1.031	1.893	167.9°
	(OH) O—H···O (PO ₄)	1.090	1.484	170.6°
2	9N—H···O (desoxyribose)	1.031	1.892	167.7°
	(OH) O—H···O (PO ₄)	1.090	1.483	170.5°
3	9N—H···O (desoxyribose)	1.031	1.890	167.2°
	(OH) O—H···O (PO ₄)	1.09	1.484	170.3°
4	9N—H···O (desoxyribose)	1.031	1.878	172.0°
	(OH) O—H···O (PO ₄)	1.085	1.503	161.9°
5	(OH) O—H···O (PO ₄)	1.091	1.480	170.7°
6	9N—H···O (desoxyribose)	1.032	1.976	175.8°
	(OH) O—H···O (PO ₄)	1.091	1.479	171.8°
7	(OH) O—H···O (PO ₄)	1.091	1.481	170.6°
8	(OH) O—H···O (PO ₄)	1.091	1.481	170.6°
9	(OH) O—H···O (PO ₄)	1.091	1.483	170.7°